



Nutrient-Induced Modifications of Wood Anatomical Traits of *Alchornea lojaensis* (Euphorbiaceae)

Susanne Spann1*, Jürgen Homeier2 and Achim Bräuning1

¹ Institute of Geography, University Erlangen-Nuremberg, Erlangen, Germany, ² Albrecht von Haller Institute of Plant Sciences, Georg August University Göttingen, Göttingen, Germany

OPEN ACCESS

Edited by:

Timothy Ian Eglinton,
ETH Zürich, Switzerland

Reviewed by:

Arthur Gessler,
WSL, Switzerland
Sabine Rosner,
Universität für Bodenkultur Wien,
Austria

*Correspondence:

Susanne Spann
susanne.spann@fau.de

Specialty section:

This article was submitted to
Biogeoscience,
a section of the journal
Frontiers in Earth Science

Received: 02 September 2015

Accepted: 15 April 2016

Published: 02 May 2016

Citation:

Spann S, Homeier J and Bräuning A
(2016) Nutrient-Induced Modifications
of Wood Anatomical Traits of
Alchornea lojaensis (Euphorbiaceae).
Front. Earth Sci. 4:50.
doi: 10.3389/feart.2016.00050

Regarding woody plant responses on higher atmospheric inputs of the macronutrients nitrogen (N) and phosphorous (P) on tropical forests in the future, an adaptive modification of wood anatomical traits on the cellular level of woody plants is expected. As part of an interdisciplinary nutrient manipulation experiment (NUMEX) carried out in Southern Ecuador, we present here the first descriptive and quantitative wood anatomical analysis of the tropical evergreen tree species *Alchornea lojaensis* (Euphorbiaceae). We sampled branch wood of nine individual trees belonging to treatments with N fertilization, N+P fertilization, and a control group, respectively. Quantitative evaluations of eleven different vessel parameters were conducted. The results showed that this endemic tree species will be able to adapt well to the future effects of climate change and higher nutrient deposition. This was firstly implied by an increase in vessel diameter and consequently a higher theo. area-specific hydraulic conductivity with higher nutrient availability. Secondly, the percentage of small vessels (0–20 μm diameter) strongly increased with fertilization. Thirdly, the vessel arrangement (solitary vessels vs. multiple vessel groupings) changed toward a lower percentage of solitary vessel fraction (V_S), and concurrently toward a higher total vessel grouping index (V_G) and a higher mean group size of non-solitary vessels (V_M) after N and N+P addition. We conclude that higher nutrient availability of N and N+P triggered higher foliage amount and water demand, leading to higher cavitation risk in larger vessels. This is counteracted by a stronger grouping of vessels with smaller risk of cavitation to ensure water supply during drier periods that are expected to occur in higher frequency in the near future.

Keywords: branch wood, evergreen tropical montane forest, Euphorbiaceae, fertilization, quantitative wood anatomy

INTRODUCTION

Besides water and light availability, temperature and salinity, the macronutrients nitrogen (N) and phosphorous (P) are considered as the most important factors controlling and limiting tree growth in the majority of the world's ecosystems (e.g., Cavelier et al., 2000; Hedin et al., 2009; Vitousek et al., 2010; Goldstein et al., 2013). Since the beginning of the industrial age, both P and N cycles have skipped out of balance due to human activities and the use of fertilizer and fossil fuel (Smil, 2000; Wright, 2005; Galloway et al., 2008). Galloway et al. (2003) described the potential effect chains of increasing reactive N within the biogeochemical cycle, stressing that especially forests have a high

potential to accumulate and transform reactive N. In particular, tropical forests will sensitively react to expected higher N and P inputs, but the full extent of their responses is discussed controversially (e.g., Tanner et al., 1990; Homeier et al., 2012; Fisher et al., 2013; Powers et al., 2015).

Goldstein et al.'s summarized (2013, p. 2) that after being released from nutrient limitation of N and P, trees will theoretically respond with higher growth rates. Additionally, the hydraulic properties can be oppositional influenced, leading to a higher xylem hydraulic conductivity, but not to a higher leaf hydraulic conductivity (efficiency of stem water supply per unit leaf surface area), although stomatal conductance will decrease to minimize water loss. Hence, it is assumed that higher nutrient availability results in a higher water deficit and this will consequently lead to more negative water potentials of fertilized trees.

These expectations result from the fact that secondary growth is directly controlled by the entire tree physiology, which in turn is compromised by external environmental factors (Fonti et al., 2010).

The vascular system (nonliving conductive cells in the xylem) of trees is responsible for the long distance water and nutrient transport from the roots to the leaves (Pittermann, 2010). However, the efficiency of the functional hydraulic properties is mainly compromised by the tradeoffs between conductivity and vulnerability to dysfunction, and has been described in detail by Tyree and Zimmermann (2002). Those tradeoffs are greatly influenced by conduit/vessel size and the arrangement and structure of the vessel network. For example, vessel grouping (min. two vessels are joined in radial or clustered groups) on the one hand increases the resilience to cavitation and might provide safety for the conductive system, but on the other hand the risk of hydraulic failure of individual vessel elements increases concurrently (Carlquist, 2001; von Arx et al., 2013). When analyzing the vascular system of branches one firstly needs to consider that trees alter their wood anatomical architecture along the axial pathway, affecting the hydraulic system from the root to the twigs differently (Tyree and Zimmermann, 2002; Sperry et al., 2008; McCulloh et al., 2010). Secondly, the wood structure of branches may differ from the stem's xylem structure, characterized by a denser, less elastic wood with a higher resistance to cavitation (Lachenbruch and McCulloh, 2014). And thirdly, tension wood is often present on the upper sides of branches which can profoundly affect the water transport due to its special kind of wood tissue, which is characterized by an internal gelatinous layer in fibers, a missing cell wall lignification, as well as fewer and smaller vessels (Barnett et al., 2014). These modifications need to be taken into account when analyzing hydraulic properties of branch wood since hydraulic functioning is controlled by mechanical demands (Fournier et al., 2014).

An increase in nutrient availability can directly influence cell formation and induce changes in vessel diameter size and arrangement (Zimmermann, 1978; Hacke, 2015). Consequently, tree species are expected to vary their hydraulic architecture due to environmental impacts, as described by Arnold and Mauseth (1999). However, studies focusing on nutrient-induced modification of wood anatomical traits are quite sparse (Harvey

and Van den Driessche, 1997; Hacke et al., 2010; Hacke, 2015) and completely lacking in tropical regions at this time (Zuidema et al., 2013). But how can those changes of the vascular system be detected or calculated? Scholz et al. (2013) provided an overview of different methodological approaches how to quantify vessel or tracheid elements in plants. Numbers of different vessel parameters help comprehending possible adaptations or changes of the xylem structure. Accordingly, comparisons with e.g., the total growth rate, the production of biomass, the foliar morphology, and foliar chemistry can be drawn (Meinzer et al., 2008; Schuldt et al., 2013; Hoeber et al., 2014).

Our investigations of the vessel system were conducted on the evergreen tropical montane tree species *Alchornea lojaensis* Secco (Euphorbiaceae). This woody species of the Euphorbiaceae is endemic in Southern Ecuador. The wood is diffuse porous and vessels range from broader solitary to rather small to mid-scale grouped radial multiples. Thus, the species is well-adapted to humid habitats, where water stress is lacking and cavitation risks are naturally minimized (Carlquist, 2001). Further, the species shows a high adaptability to nutrient-poor soil conditions, resulting in high abundance within the study forest. Therefore, we expect a high susceptibility and sensitivity to increasing availability of N and P, reflected by changes in the vessel system.

The aim of this study was to investigate to what extent or direction the vascular system of *A. lojaensis* has been changed by an increased nutrient availability of N and P, and how this affects the species' theoretical hydraulic properties. Since the tree species has been poorly studied, we carried out a descriptive wood anatomy analysis based on thin sections and common microscopic techniques. Based on the quantitative parameter "vessel lumen area," we analyzed nutrient affected modifications of vessel diameter size, theo. area-specific hydraulic conductivity, vessel grouping indices, vessel packing functions and vulnerability index. Further, we point out possible consequences for the biodiversity and the species composition of the lower tropical montane forest in Southern Ecuador.

MATERIALS AND METHODS

Study Site

The study area Reserva San Francisco (RSF, 3°58'S, 79°04'W) covers an altitudinal range from 1.600–3.140 m a.s.l. at the northern slope of the Podocarpus National Park (PNP), located in the Cordillera Real, at the eastern escarpment of the Southern Ecuadorian Andes (Richter et al., 2013). This hotspot of biodiversity hosts more than 300 tree species of which the majority belongs to the plant families Lauraceae, Melastomataceae, and Rubiaceae (Homeier et al., 2010). Local climate is described by per-humid conditions with an average annual temperature of 15.3°C and an average annual precipitation of 2067 mm at 1950 m a.s.l. (Beck and Richter, 2008). Precipitation patterns are characterized by slight seasonality. Wettest conditions are predominant from May to August, while the driest months are October and November (Rollenbeck and Bendix, 2011). During this time, rainless periods of up to more than 2 weeks may occur, potentially leading to drought stress in this otherwise per-humid environment. The

dominant soils are acid cambisols with pH values of 3.8 in the A-horizon (Wilcke et al., 2002). However, in general, soils vary considerably within the study area and are mainly nutrient-poor. Total annual atmospheric nutrient depositions are estimated to reach 14–45 kg N ha⁻¹ and 0.4–4.9 kg P ha⁻¹, respectively (Homeier et al., 2013).

Experimental Design and Branch Sample Design

Our study was carried out within an interdisciplinary, full-factorial nutrient manipulation experiment located inside the RSF at an altitude between 2020 and 2120 m a.s.l. (abbreviated “NUMEX,” in the following, for details see Homeier et al., 2012). The fertilization experiment (**Figure 1**) was set up in a randomized, fourfold replicated block design, each consisting of four different treatments (N, P, N+P, and unfertilized control, 20 × 20 m plots per treatment). Nutrient applications started in 2008 and were repeated biannually. Total amounts of 50 kg ha⁻¹ yr⁻¹ of N (as urea), 10 kg ha⁻¹ yr⁻¹ of P (as NaH₂PO₄·2H₂O) and the combination of both (N+P plots) were added on the respective plots (Homeier et al., 2013).

A. lojaensis Secco (Euphorbiaceae) is one of the most common tree species within the NUMEX plots, with an average annual stem diameter growth of 0.12 mm (unfertilized control, monitoring period: February 2008–January 2009, Homeier et al., 2012).

Forty-one species of the genus *Alchornea* are distributed along the pan-tropics, with a majority in Central and South America (Secco, 2008). However, *A. lojaensis* is one of the very few endemic species, being restricted to the Zamora-Chinchi province (southern Ecuador) between elevations of 1900–2400 m a.s.l. (Homeier and Werner, 2008). Although, the evergreen broadleaved tree species *A. lojaensis* has been described morphologically by Secco (2008), neither its wood structure nor its wood anatomical parameters have been studied so far.

In February 2013, five years after the start of the fertilization experiment, we collected one branch sample per tree of nine *A. lojaensis* individuals within three different treatments of the NUMEX plots (Control, N and N+P). Within each treatment, three individual trees were sampled. In this study, specimens of P plots were not investigated due to technical difficulties regarding the thin-section preparation.

Xylem Anatomical Measurements

Wood anatomical measurements and hydraulic calculations were performed on cross-sections of the collected branch samples. Each branch specimen was dehydrated with increasing ethanol concentration series and rotihistol, embedded in paraffin and cut into thin-sections (10 μm) with an electronic rotation microtome (Leica, Germany). All transverse sections, cleaned of residual paraffin, were stained with a mixture of Fuchsin, Chrysoidin and Astra blue (FCA solution after Etzold, 2002) and finally fixed with Canada balsam.

Digital photos with a fourfold magnification (Leica, microscopic system) were taken and merged together to analyze the entire xylem area, assuming that the complete area is conductive. To simplify subsequent measurements, vessel lumen was manually edited by using Adobe Photoshop. While solitary

vessels were colored red, grouped vessels remained white. We divided every cross-section into four parts (through the pith) to achieve faster measurement and to provide a better measurement accuracy.

Vessel Diameter and Hydraulic Calculations

WinCELL 2010a software (®Regents, Canada) was used to measure vessel lumen cross sectional area (VA, μm²) of each single vessel. Vessel area was converted to an idealized arithmetic vessel diameter (d , μm) assuming circularity of vessels (Scholz et al., 2013). Based on each single arithmetic vessel diameter (d), we calculated the hydraulic vessel diameter (d_h , μm, Equation 1) according to Tyree and Zimmermann (2002) as:

$$d_h = \left(\frac{\sum d^4}{n} \right)^{\frac{1}{4}} \quad (1)$$

The theoretical hydraulic conductivity (k_h^{theo} , m⁴MPa⁻¹ s⁻¹) was evaluated from the vessel radii (r , μm) using the Hagen-Poiseuille law (Equation 2, modified after Tyree and Zimmermann, 2002), where η is the viscosity of water, calculated at 20.0°C.

$$k_h^{theo} = \frac{\pi \sum r^4}{8\eta} \quad (2)$$

Subsequently, we determined the theo. area-specific hydraulic conductivity (k_s^{theo} , kg m⁻¹MPa⁻¹ s⁻¹, Equation 3) by including the density of water (ρ) at 20.0°C (Tanaka et al., 2001), and dividing it by the total xylem area (A_{xylem}).

$$k_s^{theo} = \frac{k_h^{theo} \rho}{A_{xylem}} \quad (3)$$

Vessel Frequency and Vulnerability Index

To determine vessel frequency (VF, average number of vessels per mm²), 10 segments with an area of 1 mm² were randomly selected on each cross section and all vessels were counted as individuals (Wheeler, 1986). Based on the arithmetic vessel diameter (d) and the number of vessels per mm², we calculated the averaged area-weighted vessel diameter (d_a ; μm) for each field by using Equation 4 and computed the maximum vessel packing limit, assuming square packing (McCulloh et al., 2010, 2011).

$$d_a = \left(\frac{\sum d^2}{n} \right)^{0.5} \quad (4)$$

Vessel frequency per mm² and area-weighted vessel diameter were also used to calculate the vessel vulnerability index (VI; Carlquist, 1977; **Table 2**). The ratio of these two variables offers a rough assessment about the trees' sensitivity to the risks of cavitation or embolism.

Vessel Arrangement and Vessel Indices

Table 1 provides an overview of three different indices that were defined to quantify vessel groupings. To achieve optimal results,

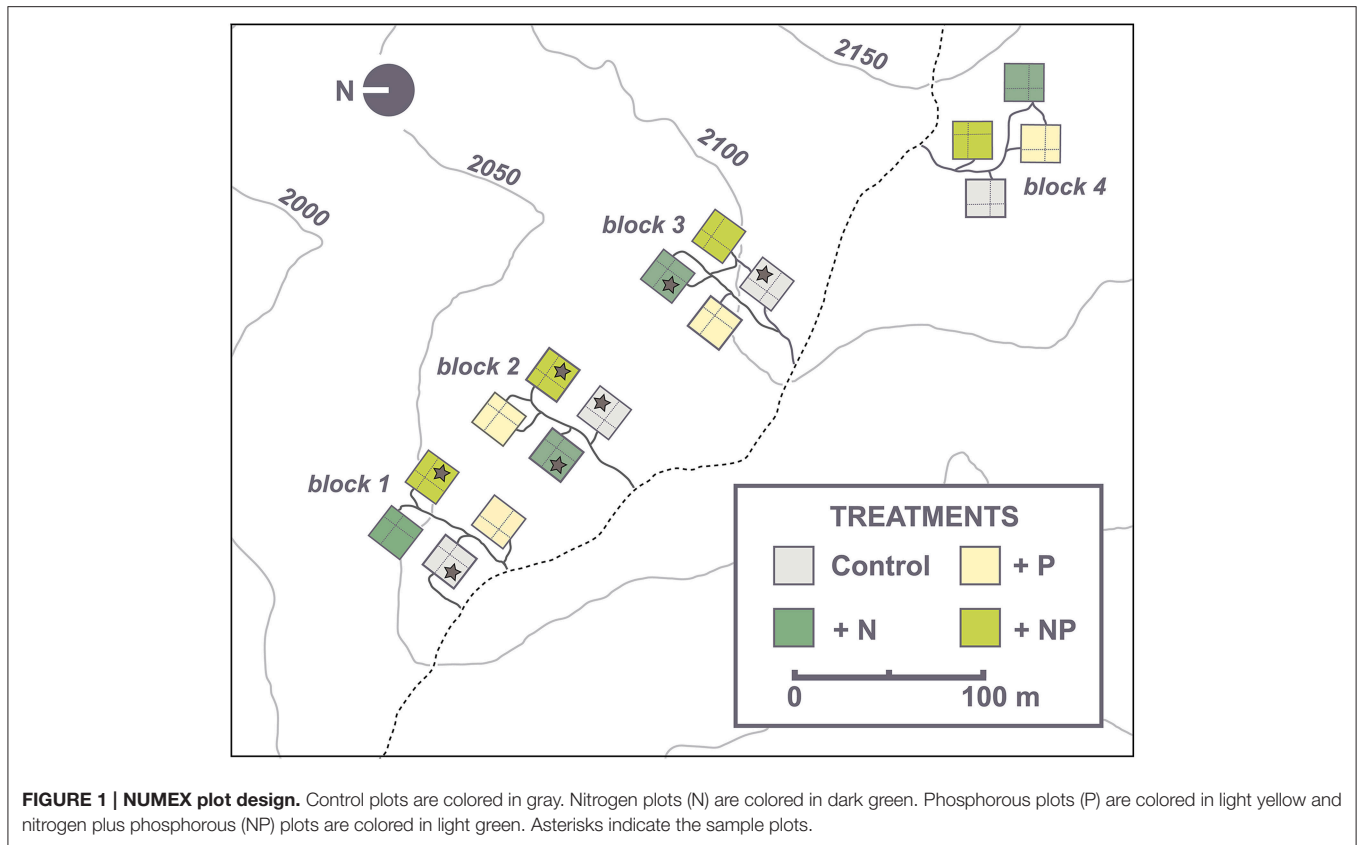


TABLE 1 | Index, ratio, definition, and references of different vessel grouping indices.

Index	Ratio	Definition	References
Vessel grouping index (V_G)	$\frac{N_{vessels}}{N_{groupings}}$	Mean number of vessels per group	Carlquist, 2001
Vessel solitary index (V_S)	$\frac{N_{solitary\ vessels}}{N_{vessels}}$	Ratio of solitary vessels to all vessels	Scholz et al., 2013; von Arx et al., 2013
Vessel multiple index (V_M)	$\frac{N_{multiple\ vessels}}{N_{multiple\ groupings}}$	Mean group size of non-solitary vessels	Scholz et al., 2013; von Arx et al., 2013

it was necessary to count every vessel separately, based on the total xylem area (Wheeler, 1986). Additionally, we evaluated the vessel frequency distribution (absolute and relative) of different vessel group sizes (von Arx et al., 2013).

Statistical Methods

All statistical analyses were performed with IBM® SPSS® Statistics Version 23. All calculations of the mean values were performed at the tree level [$n = 3$ (C): 3 (N): 3 (N+P)]. Requirements for normal distribution and statistical methods were checked with the Shapiro Wilk test and also visually (histogram). For confirming homogeneity of variance we used the Levene Test. In case of variance heterogeneity, significance threshold was increased to 0.01 (Bühl, 2008).

Treatment effects on different wood anatomical parameters (arithmetic vessel diameter, hydraulic vessel diameter, theo. area-specific hydraulic conductivity, vessel frequency, vulnerability index, and vessel indices) were conducted on the tree mean values and compared in a univariate ANOVA (factor 1 = treatment) with a Scheffé *post-hoc* test. Vessel arrangements effects (solitary vessels vs. multiple vessels) on arithmetic vessel diameter differentiated into treatments were tested with an unpaired student-*t*-test. To evaluate the influence of the combination of these two variables on vessel anatomical parameters we performed a multivariate analysis of variance (factor 1 = treatment; factor 2 = vessel arrangement) including η^2 effect size of the model. To show the relationship between vessel frequency and area-weighted diameter between the different treatments we performed a linear regression at the single tree level ($n = 10$ per tree; $n = 30$ per treatment). The corresponding means were compared at the tree level.

RESULTS

Descriptive Analysis of Wood Anatomical Traits of *Alchornea lojaensis*

Distinctness of growth ring boundaries (GRB, marked by arrows) dramatically differed along the whole branch xylem area. At several points, GRBs are clearly visible by flattened and thickened libriform fibers (LF, **Figures 2A,B**). However, a continuous, clear “tree ring” boundary could not be detected. Typically for

TABLE 2 | Mean percentage ratio between solitary vessels and multiple vessels, mean vulnerability index (VI), and mean vessel grouping indices for all three treatments.

Treatment	n	Percentage ratio				VI		Vessel grouping indices					
		Solitary vessel		Multiple vessels		M	SD	V_G		V_M		V_S	
		M	SD	M	SD					M	SD	M	SD
C	3	30.80	3.87	69.20	3.87	4.02	1.67	1.92	0.10	3.26	0.10	0.31	0.03
N	3	26.80	2.69	73.20	2.69	7.31	4.07	2.07	0.14	3.36	0.23	0.27	0.02
N+P	3	30.00	8.52	70.00	8.52	6.23	2.97	2.02	0.32	3.49	0.50	0.30	0.09

C, Control; N, Nitrogen; N+P, Nitrogen + Phosphorous; n, sample size; M, mean value; SD, standard deviation; VI, Vulnerability Index; V_G , Vessel grouping index; V_S , Vessel solitary index; V_M , Vessel multiple index; Means were calculated at the tree level.

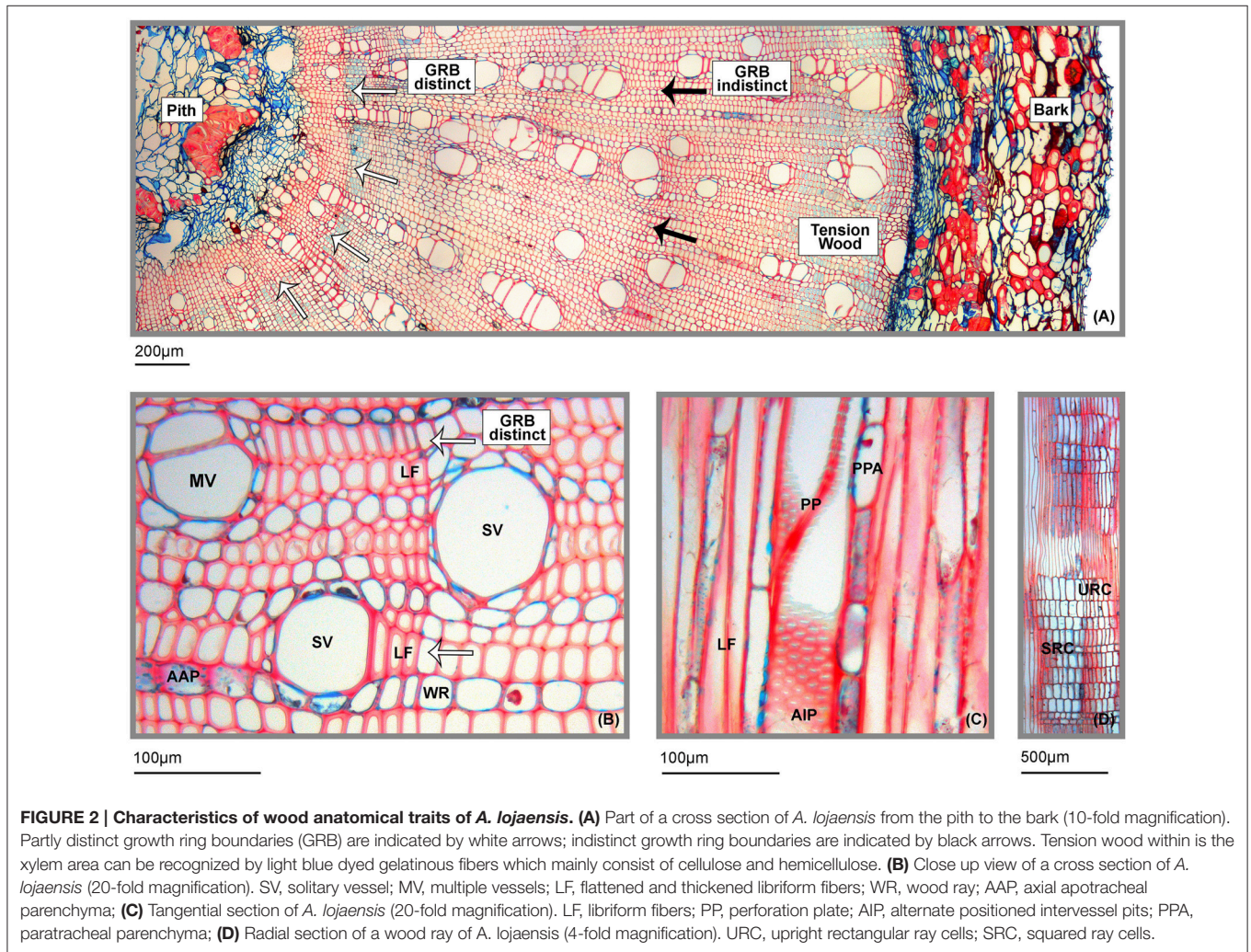


FIGURE 2 | Characteristics of wood anatomical traits of *A. lojaensis*. (A) Part of a cross section of *A. lojaensis* from the pith to the bark (10-fold magnification). Partly distinct growth ring boundaries (GRB) are indicated by white arrows; indistinct growth ring boundaries are indicated by black arrows. Tension wood within is the xylem area can be recognized by light blue dyed gelatinous fibers which mainly consist of cellulose and hemicellulose. (B) Close up view of a cross section of *A. lojaensis* (20-fold magnification). SV, solitary vessel; MV, multiple vessels; LF, flattened and thickened libriform fibers; WR, wood ray; AAP, axial apotracheal parenchyma; (C) Tangential section of *A. lojaensis* (20-fold magnification). LF, libriform fibers; PP, perforation plate; AIP, alternate positioned intervessel pits; PPA, paratracheal parenchyma; (D) Radial section of a wood ray of *A. lojaensis* (4-fold magnification). URC, upright rectangular ray cells; SRC, squared ray cells.

branch wood of dicots, we found several parts of tension wood within the xylem area which can be recognized by blue dyed gelatinous fibers whose cell walls mainly consist of cellulose and hemicellulose (Figure 2A).

The wood is diffuse-porous, consisting of both, one third of solitary vessels (SV, $M = 29.2\%$, $SD = 2.12$) and two third of radial multiple vessels (MV, $M = 70.8\%$; $SD = 2.12$). Most of the multiples comprise short rows consisting of 2–5

vessels; however, maximum row numbers can reach up to 10–15 vessels (Figure 2A). Vessel outlines are rounded with a scanty paratracheal parenchyma (PPA, Figure 2C). Intervessel pits are positioned alternately (AIP, Figure 2C); perforation plates (PP, Figure 2C) are simple and diffuse; apotracheal axial parenchyma (AAP, Figure 2B) is distinct. Wood stability is provided by non-septated libriform fibers (LF, Figures 2A,B). Vascular or vascentric tracheids are absent. Wood rays (WR, Figures 2B,D)

are exclusively uniseriate and hetero-cellular, composed of upright rectangular (URC, **Figure 2D**) and squared ray cells (SRC, **Figure 2D**). Radial canals are occasionally present in rays.

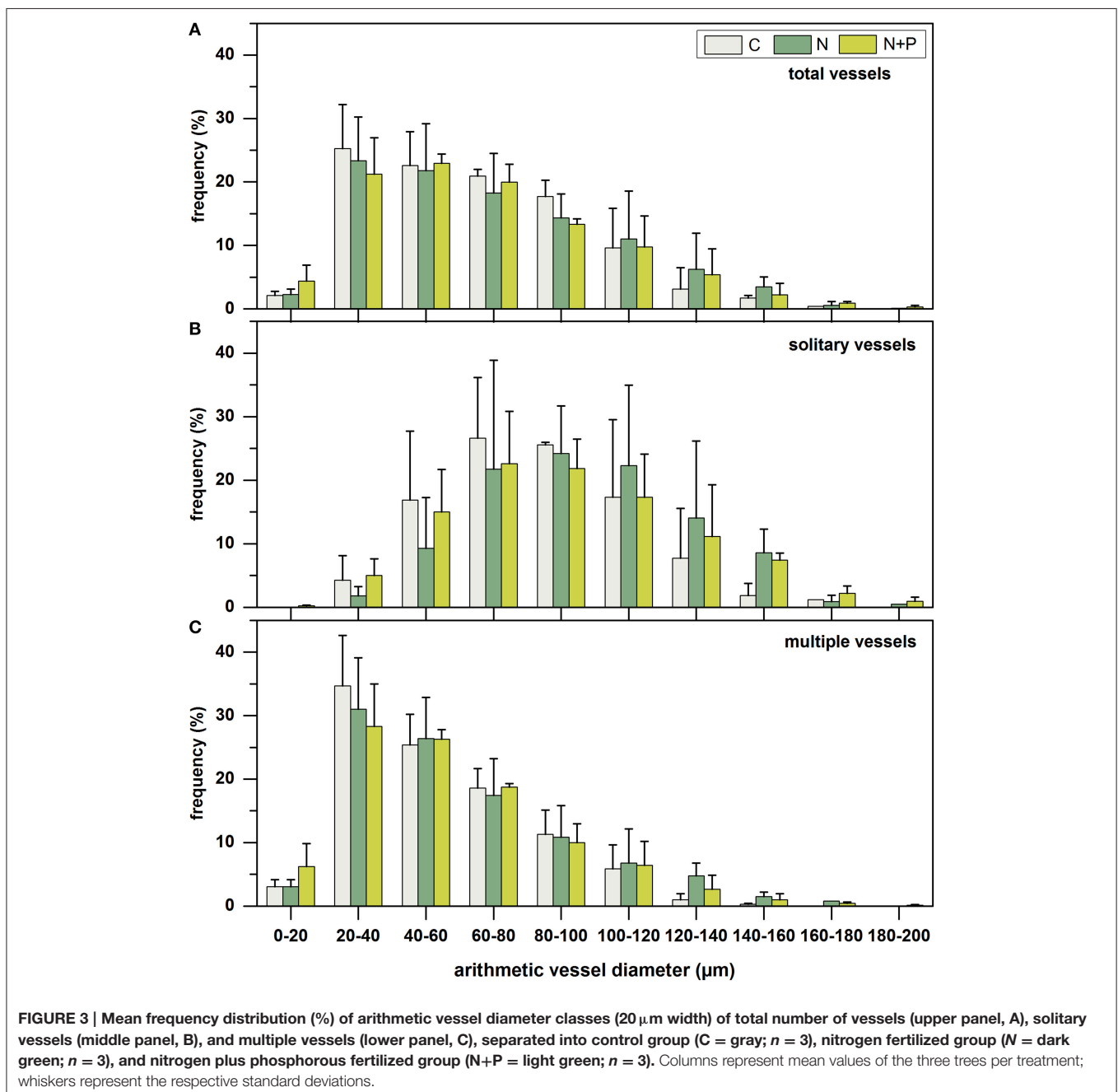
Quantitative Analysis of Wood Anatomical Traits of *Alchornea lojaensis*

Arithmetic Vessel Diameter: Distribution and Means

The analyses of the percentage ratio between solitary vessels and multiple vessels obtained slightly diverging results for the individual treatments (**Table 2**), indicating a comparatively smaller proportion of solitary vessels after N addition compared

to the C and N+P treatments. However, differences were not statistically significant [$F_{(2, 6)} = 0.424, \rho = n.s.$].

Striking different frequency distribution patterns of vessel diameter classes (20 μm width) existed for total (**Figure 3A**), solitary (**Figure 3B**), and multiple vessels (**Figure 3C**). While solitary vessels were almost normally distributed, frequency of multiple vessels decreased linearly from small (20–40 μm) to large (180–200 μm) diameter classes. Considering exclusively solitary vessels, smaller arithmetic vessel diameters between 60 and 80 μm appeared most frequently for C and N+P, whereas highest frequency between 80 and 100 μm occurred after N-fertilization. Regarding the frequency distribution of



multiple vessels, highest incidence could be found for small vessel diameters between 20 and 40 μm for all treatments. The frequency of the smallest diameter class between 0 and 20 μm clearly increased after N and N+P addition compared to the control samples.

Figure 4 illustrates that fertilization also slightly affected mean arithmetic vessel diameter size. For the case of all vessels, N-addition ($M = 68.16$, $SD = 12.91$) caused larger means than the combination of N+P ($M = 66.67$, $SD = 10.70$) or no fertilization ($M = 63.48$, $SD = 9.73$), although not statistically significant. A similar inter-treatment pattern was also seen for exclusively solitary vessels (control: $M = 83.14$, $SD = 14.69$; nitrogen $M = 94.94$, $SD = 17.07$; nitrogen + phosphorous $M = 88.93$, $SD = 14.15$) and multiple vessels (control: $M = 54.48$, $SD = 7.09$; nitrogen $M = 58.20$, $SD = 10.24$; nitrogen + phosphorous $M = 57.08$, $SD = 8.97$), respectively. Whereby, the effect of fertilization was higher for solitary vessels.

The intra-treatment comparison showed that vessel arrangement had a significant effect on vessel diameter size, which was expressed by significantly larger diameters of solitary vessels than of multiple vessels. (control [$t_{(4)} = 3.034$, $\rho < 0.05$], nitrogen [$t_{(4)} = 3.196$, $\rho < 0.05$], and nitrogen + phosphorous [$t_{(4)} = 3.293$, $\rho < 0.05$]).

The two-way ANOVA reaffirmed that treatment effect [factor 1, $F_{(2, 18)} = 0.0576$, $\rho = \text{n.s.}$, $\eta^2 = 0.008$) and the effect of vessel arrangement [factor 2, $F_{(1, 18)} = 30.076$, $\rho < 0.001$, $\eta^2 = 0.715$] on vessel diameter size, whereby the latter had a substantially greater effect. An interaction between these two factors could not be determined [$F_{(2, 18)} = 0.158$, $\rho = \text{n.s.}$, $\eta^2 = 0.026$].

Hydraulic Vessel Diameter and Theoretical Area-Specific Hydraulic Conductivity (k_s^{theo})

Inter-treatment comparison showed slightly different patterns of the mean hydraulic vessel diameter (**Table 3**), indicating larger diameters after fertilization. Consequently, N and N+P fertilization led to an increasing k_s^{theo} for all vessels, for solitary vessels as well as for multiple vessels. However, k_s^{theo} conductivity was highest for the N+P samples. Astoundingly, multiple vessels of the N+P group ($0.89 \cdot 10^{-2} \text{ m}^2 \text{ MPa}^{-1} \text{ s}^{-1}$) reached similar k_s^{theo} like solitary vessels of the control group ($0.92 \cdot 10^{-2} \text{ m}^2 \text{ MPa}^{-1} \text{ s}^{-1}$), indicating that the high number of small diameter multiple vessels (N+P) can compensate for susceptibility to extreme climatic events like droughts. This also means that the high k_s^{theo} of total vessels for all treatments was a result of the high number of smaller vessels.

Vessel Frequency and Vulnerability Index

An apparent, significant converse relationship between area-weighted vessel diameter and vessel frequency was found for every single treatment (**Figure 5**), basically signifying that the larger the area-weighted diameter of a vessel, the fewer number of vessels could fit into 1 mm^2 ($p < 0.5$). However, the slope of the regression functions was steeper for the control treatment than for the fertilized treatments.

Mean area-weighted diameters were larger after fertilization compared to the control (**Figure 5**), but, although mean area-weighted diameters after N and N+P addition were nearly the same, fewer vessels were packed in a given area after fertilization

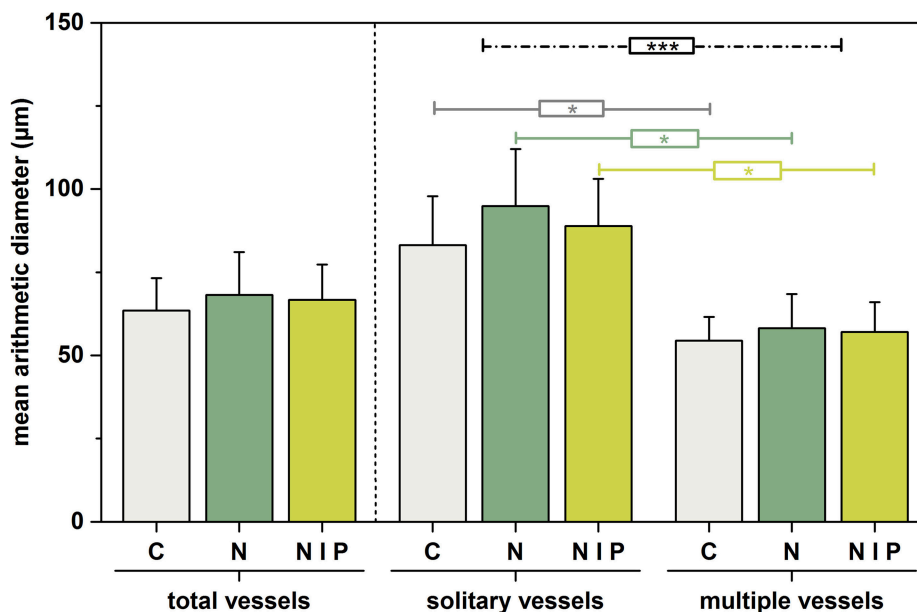


FIGURE 4 | Alteration of mean arithmetic vessel diameter size in response to fertilization for the total number of vessels (left panel) and for solitary and multiple vessels (middle and right panel). Columns represent mean values of the three trees per treatment; whiskers represent the respective standard deviations. Corresponding colored lines mark significant inter-treatment comparisons due to vessel arrangement (Student $-t$ -test). Black line marks significant difference between vessel arrangements as a result of Two-way ANOVA. Significance levels are marked by * $p < 0.05$, *** $p < 0.001$. C, control, gray; $n = 3$; N = nitrogen, dark green, $n = 3$; N+P = nitrogen + phosphorous, light green, $n = 3$.

TABLE 3 | Mean hydraulic vessel diameter (μm) and theo. area-specific hydraulic conductivity [k_s^{theo} ($\text{m}^2 \text{MPa}^{-1} \text{s}^{-1} 10^{-2}$)] differentiated into vessel arrangement and treatment.

Vessel arrangement	Treatment	Hydraulic vessel diameter (μm)			Theo. area-specific hydraulic conductivity [k_s^{theo} ($\text{m}^2 \text{MPa}^{-1} \text{s}^{-1} 10^{-2}$)]	
		<i>n</i>	<i>M</i>	<i>SD</i>	<i>M</i>	<i>SD</i>
Total vessel	C	3	79.27	11.67	1.63	0.28
	N	3	85.93	17.41	1.73	0.79
	N+P	3	86.60	14.58	1.98	0.43
Solitary vessels	C	3	92.32	14.59	0.92	0.19
	N	3	103.20	18.58	0.97	0.43
	N+P	3	101.77	17.25	1.10	0.21
Multiple vessels	C	3	70.05	8.92	0.71	0.26
	N	3	75.67	16.01	0.76	0.36
	N+P	3	76.53	13.29	0.89	0.44

C, Control; N, Nitrogen; N+P, Nitrogen + Phosphorous; *n*, sample size; *M*, mean value; *SD*, standard deviation; Means were calculated at the tree level.

with N and caused the highest concomitant reduction of vessel frequency.

These results were strengthened by the vulnerability index. VI values varied considerably between treatments (Table 2) although not statically significant. After fertilization, vessel diameters were larger than those of the control group, but also showed a considerable increase of the vulnerability index, causing a higher susceptibility to environmental changes.

Vessel Indices and Vessel Group Sizes

Insignificant differences in vessel indices were determined between the treatments (Table 2). However, after fertilization, V_G and V_M tended to increase while the control samples showed highest proportions of solitary vessels (V_S). That apparent relationship suggested that nutrient addition caused more grouped, but fewer and larger solitary vessels. Unfortunately, due to the relative small sample size and resulting low degrees of freedom, correlations could not be verified statistically.

Relative frequency of different group sizes also varied between treatments. Table 4 shows the absolute numbers of the vessel group sizes for each sample as well as the percentage mean values at the tree level with the respective standard deviation. In all treatments, more than 50% of the vessel groupings consisted of solitary groupings, showing the smallest proportion for after N fertilization. However, N fertilization affected group sizes between 2 and 6 vessels, whereas the combination of N+P resulted in the development of groupings with more vessel elements.

DISCUSSION

Descriptive Analysis of Wood Anatomical Traits of *Alchornea lojaensis*

Woody species of Euphorbiaceae show vessel arrangements ranging from solitary to multiple vessels in double-digit range

and present libriform fibers as imperforate tracheary elements (Carlquist, 1984). By counting each vessel individually, we could affirm this pattern for *A. lojaensis*, with about 31% solitary vessels and 69% multiple vessels for the unfertilized trees (Table 2). Strong visual similarities in wood structure were found with *A. grandiflora* and *A. pearcei* from Brazil (Chavarri and Léon, 2005).

Contrary to the evergreen species *A. sidifolia* from Brazil (Filho et al., 2004), we could not detect distinct increment zones in our studied branch samples of *A. lojaensis* (Figures 2A–D). Although flattened and thickened libriform fibers were detected for both species, a distinct continuous band of radially flattened and thickened fibers marking a growth boundary was not found in branches of *A. lojaensis*. The same applies to the closely related species *A. triplinervia*, also occurring within the study area and in South Brazil (Homeier and Werner, 2008). The different wood anatomical properties might be explained by different growth strategies related to climatic differences between the two ecosystems (Worbes, 1995). While a distinct dry period between June and August with less than 60 mm precipitation per month might induce cambial dormancy accompanied by anatomically visible increment zones of the Brazilian species (Filho et al., 2004), *A. lojaensis* is well-supplied by soil water the whole yearlong. Therefore, the whole xylem area of the branches is assumed to be completely conductive. This assumption was further supported by the fact that tyloses were not observed.

Arithmetic Vessel Diameter: Distribution and Means

In order to assess the full extent of vessel anatomy variability of *A. lojaensis* affected by nutritional impacts, we compared the results for the control group with a study from Schuldt (2005), which was carried out within the same research area (PNP, without fertilization). In that study, mean vessel diameter of different twigs measured $41.04 \mu\text{m}$ at an elevation of 1890 m a.s.l. In our study, *A. lojaensis* reached 155% larger mean vessel diameter ($M = 63.48$, $SD = 9.73$) at almost the same elevation (Figure 4). However, one needs to consider the generally decreasing size of vessels from stems to twigs (Tyree and Zimmermann, 2002). Nevertheless, those values can still be classified as vessels with rather small to average diameter size (Wheeler et al., 1989).

N and N+P fertilization triggered changes in vessel size, with a tendency toward larger diameters (Figure 4). This confirms observations for hybrid poplar, where an increase of N and/or P availability was reported to enhance vessel diameter in stems (Harvey and Van den Driessche, 1997; Hacke et al., 2010; Hacke, 2015). However, inverse responses of vessel diameter size after nutrient addition were also found (e.g., Arnold and Mauseth, 1999; Faustino et al., 2013). Such diverging fertilization effects resulted mostly from different elevations, soil types, or tree species.

Besides treatment effects, the vessel arrangement of *A. lojaensis* revealed a high impact on vessel diameter size, which is consistent with findings of Arnold and Mauseth (1999) for *Cereus peruvianus* and *Cereus tetragonus*. Hence, this effect is important to be considered when analyzing diffuse porous

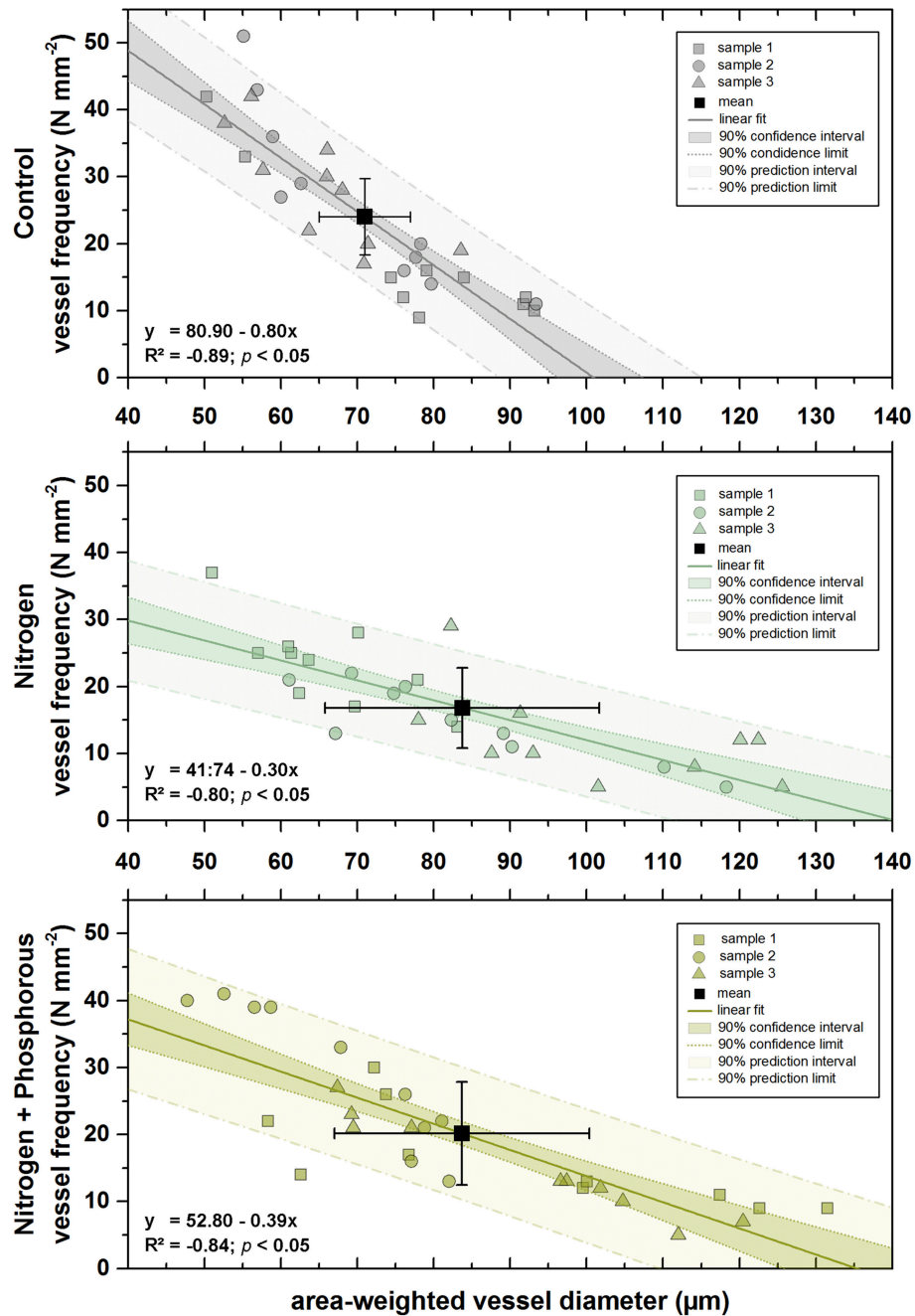


FIGURE 5 | Regression models between area-weighted diameter (μm) and vessel frequency ($N\text{ mm}^{-2}$) of different fertilization treatments. Upper panel = control treatment; values of sample 1, 2, and 3 are marked by gray rectangles, circles, and triangles, respectively ($n = 10$ in each case). Mean value of all samples ($n = 3$) is marked by the black rectangle ($n = 10$), respective standard deviations are marked by black whiskers. Regression model: gray continues line indicates the linear fit, gray dotted lines indicate 90% confidence limits, gray dot-dashed lines indicate 90% prediction limits. Middle panel = nitrogen treatment; values of sample 1, 2, and 3 are marked by dark green rectangles, circles, and triangles, respectively ($n = 10$ in each case). Mean value of all samples ($n = 3$) is marked by the black rectangle ($n = 10$), respective standard deviations are marked by black whiskers. Regression model: dark green continues line indicates the linear fit, dark green dotted lines indicate 90% confidence limits, dark green dot-dashed lines indicate 90% prediction limits. Lower panel = nitrogen + phosphorous treatment; values of sample 1, 2, and 3 are marked by light green rectangles, circles, and triangles, respectively ($n = 10$ in each case). Mean value of all samples ($n = 3$) is marked by the black rectangle ($n = 10$), respective standard deviations are marked by black whiskers. Regression model: light green continues line indicates the linear fit, light green dotted lines indicate 90% confidence limits, light green dot-dashed lines indicate 90% prediction limits. Respective regression equations with significance values are shown in each panel, respectively.

TABLE 4 | Absolute numbers and mean relative frequency distribution of vessel group size.

Treatment	Vessel group size															Total number of groupings		
	1	2	3	4	5	6	7	8	9	10	11	12	13	14	15			
C	Sample 1	n	594	152	105	59	24	13	6	3	4	–	–	1	–	–	–	961
	Sample 2	n	215	82	40	30	18	7	8	1	–	–	–	–	–	–	–	401
	Sample 3	n	561	152	87	45	24	14	11	3	–	4	3	1	2	1	–	908
	<i>M</i>	%	59.07	17.63	10.17	6.20	3.20	1.53	1.27	0.27	0.13	0.13	0.10	0.07	0.07	0.03	0.00	
	<i>SD</i>		4.73	2.44	0.67	1.25	1.13	0.15	0.70	0.06	0.23	0.23	0.17	0.06	0.12	0.06	0.00	
N	Sample 1	n	286	92	55	45	24	17	6	6	3	3	2	–	–	–	–	539
	Sample 2	n	448	151	89	55	29	14	7	4	–	–	1	–	–	1	–	799
	Sample 3	n	430	134	105	47	31	18	5	1	1	–	1	–	–	–	–	733
	<i>M</i>	%	54.93	17.77	11.63	7.10	4.03	2.43	0.87	0.57	0.27	0.20	0.20	0.00	0.00	0.03	0.00	
	<i>SD</i>		1.61	0.99	1.76	1.11	0.45	0.71	0.25	0.50	0.29	0.35	0.17	0.00	0.00	0.06	0.00	
N+P	Sample 1	n	363	136	98	60	42	18	12	6	2	4	1	1	3	–	1	746
	Sample 2	n	532	74	96	48	31	19	12	8	1	5	1	1	–	2	1	831
	Sample 3	n	415	125	44	35	7	9	3	4	1	1	–	–	–	–	–	644
	<i>M</i>	%	59.03	15.50	10.50	6.40	3.47	2.03	1.17	0.80	0.20	0.43	0.07	0.07	0.10	0.07	0.07	
	<i>SD</i>		8.95	5.75	3.29	1.40	2.26	0.55	0.59	0.20	0.10	0.21	0.06	0.06	0.17	0.12	0.06	

Absolute numbers are based on the single tree level. Mean values (in %) are based on the mean tree level ($n = 3:3:3$). Total number of groupings is calculated by the sum of all groupings, based on the tree level. C, Control; N, Nitrogen; N+P, Nitrogen + Phosphorous; n, absolute number of groupings; *M*, mean.

wood, since potential fertilization effects might be masked when vessels of different grouping size are analyzed together. Only by analyzing multiple and solitary vessels separately, the full effect of fertilization on vessel arrangement will become apparent, likewise we could find a slightly stronger influence on solitary vessels.

Theoretical Area-Specific Hydraulic Conductivity (k_s^{theo})

Changes in vessel diameter size generally provide inferences about the potential radial growth rates of trees, since larger vessels have a higher k_s^{theo} and consequently ensure increased water supply to support enhanced transpiration and photosynthetic rates (e.g., Meinzer et al., 2008, 2010; Smith et al., 2013; Hoeber et al., 2014; Oladi et al., 2014). The relation between higher growth capacity and vessel size becomes understandable, considering that the theo. hydraulic conductivity is related to the fourth power of the vessel radius (Tyree and Zimmermann, 2002). For *A. lojaensis* we calculated a high k_s^{theo} of $1.63 \cdot 10^{-2} \text{ m}^2 \text{ MPa}^{-1} \text{ s}^{-1}$ at 20.0°C at the control site (Table 3). However, twigs examined by Schuldt (2005) reached computed theo. values of $2.2 \cdot 10^{-2} \text{ m}^2 \text{ MPa}^{-1} \text{ s}^{-1}$ within the same study area. Both results can be classified as rather high values k_s^{theo} which appears to have been due to the fact, that all calculations were based on idealized vessel diameters and do not correspond to physically ideal circular capillaries.

Fewer but larger vessels are regarded to be more efficient in water and nutrient transport than more, but narrow vessels (Zanne et al., 2010). Therefore, due to N and N+P fertilization, k_s^{theo} of *A. lojaensis* was expected to increase to the same extent,

as it was the case for arithmetic vessel diameter (Tyree and Zimmermann, 2002). However, k_s^{theo} tended to increase most strongly after N+P fertilization, most probably resulting from higher V_m (Table 2) compared to N fertilization.

Vessel Frequency, Vulnerability Index, and Vessel Grouping

Coincidentally with increasing area-weighted vessel diameter, vessel frequency decreased. This inverse relationship is often found in wood anatomical studies (e.g., Zimmermann, 1978; Tyree and Zimmermann, 2002; McCulloh et al., 2010, 2011; Schuldt et al., 2013). Although the area-weighted vessel diameter might not reflect real measurements, N ($M = 83.74$, $SD = 17.95$) and N+P ($M = 83.67$, $SD = 16.68$) fertilized samples had nearly the same mean area-weighted vessel diameters (Figure 5). However, the combination of both nutrients ($M = 20.17$, $SD = 7.67$) lead to about 20% more vessels in the xylem than after N addition ($M = 16.83$, $SD = 5.99$). Thus, *A. lojaensis* probably compensates smaller solitary vessel diameters by a higher packing of grouped vessels after N+P addition.

The relationship between vessel frequency, vulnerability, resistance to cavitation, and hydraulic conductivity is relatively well-understood and several studies examined the trade-off between efficiency and safety (e.g., Hacke et al., 2006; Sperry et al., 2008; Zach et al., 2010). At first glance, the quite high vulnerability index of fertilized *A. lojaensis* samples suggests that this species is highly susceptible for environmental risks (Table 2). However, branch wood is typically denser than stem wood, and vessels are often reduced and narrower due to tension wood, resulting in higher embolism resistance (Lachenbruch and

McCulloh, 2014). This is substantiated by our investigations on the drought sensitivity of *A. lojaensis* using dendrometers (Homeier et al., 2013; Spannl et al., 2013). Despite several dry spells of four to nine consecutive rainless days, the daily amplitude of stem diameters showed no significant difference between fertilized and non-fertilized *A. lojaensis* tree individuals. Carlquist (1977, 2001) postulated that vessel groupings, in particular radial multiples, provide safety against cavitation by taking over the function of earlier formed vessels without alteration of the conductive system. For instance, if a vessel within a group is blocked by embolism, the other remaining vessels can maintain the axial water transport, thus decreasing drought vulnerability.

A higher degree of vessel grouping can be attained by a decrease in solitary vessels and larger groups of vessel multiples (von Arx et al., 2013). Confirming that hypothesis, we determined a decrease in V_S and an increase in V_G and V_M after addition of N and N+P in *A. lojaensis*. Hence, other vessel anatomical traits like, e.g., intervessel pit membrane structure or perforation pits are possibly responsible to provide more safety in the hydraulic system of angiosperms and also conifers (Tyree and Zimmermann, 2002; Cochard et al., 2009; Smith et al., 2013). Overall, despite the high vulnerability values, the risk of hydraulic failure for *A. lojaensis* at our study site can be deemed as rather small, because the per-humid conditions considerably minimize water stress, and risks of freezing or excessive heating are not given. However, these results have to be assessed with care due to the fact that the vulnerability Index was based on the diameter and not measured by a (t/b) ratio (t = wall thickness, b = lumen diameter, Hacke, 2015).

Wood Anatomy and Physiological Functioning

In tropical and subtropical forests, physiological functioning and stem growth are closely related to hydraulic and anatomical properties of the wood as well as to foliar chemistry and leaf morphological traits (e.g., Fichtler and Worbes, 2012, for a summary; Mayor et al., 2014). Homeier et al. (2012, 2013) examined total growth rates and leaf morphology of fertilized and non-fertilized *A. lojaensis* within the same study plots. After one year of fertilization (February 2008–January 2009), increasing stem diameter increment rates were already detected after N (+33%) and N+P fertilization (+42%, Homeier et al., 2012). However, increment rates were higher after the fifth year (N: +56%; N+P: +95%, Homeier, personal communication). Thus, not exclusively the vessel diameter, but also the k_s^{theo} might predict a potential maximal diameter growth rates (Fan et al., 2012). Specific leaf area and foliar N concentration of *A. lojaensis* increased after adding N and N+P (Homeier et al., 2012), indicating thinner but larger and less long-lived leaves (Poorter et al., 2009). Since foliar N concentration and photosynthetic capacity are directly related, fertilization is expected to also increase photosynthetic rates and related water demand (Wright et al., 2004; Homeier et al., 2012). As a consequence, increasing nutrient availability can trigger more negative water potentials

under drought stress (Goldstein et al's., 2013) and hence to a higher risk of vessel cavitation.

CONCLUSION

In this study, alterations of wood anatomical patterns of *A. lojaensis* induced by fertilization effects were detected. After the fertilization with N and N+P, increasing changes in arithmetic and hydraulic vessel diameter, k_s^{theo} , mean group size of non-solitary vessels and vulnerability index were found. Concomitantly, we found a decrease in vessel frequency as well as a lower V_S and an increasing V_G , triggered by higher nutrient availability. Our findings agree with Goldstein et al's. (2013) postulate about the effects of the macronutrients N and P on forest ecosystems. Accordingly, even moderate depositions of airborne N and P can cause striking changes in the structural features of tropical montane forests. We are not able to classify the main limiting nutrient to this tree species and ecosystem, since effects of P fertilization were not analyzed specifically.

However, we were able to detect that the effects of N and N+P are species specific. Tree species less common within the study area mostly “profited” from additional nutrients (Spannl et al., 2013) whereas more abundant species reduced their growth rates at the same time. *A. lojaensis* seems to be able to adapt well to expected effects of climate change in the study area due to major modifications of the vascular system. Therefore, it is expected that this tree species will become more abundant in this ecosystem in South Ecuador under future changing climatic conditions. However, to understand the complexity of the nutrient cycles of N and P and the responses of tropical forests, more long-term experiments like this study in Southern Ecuador are needed.

AUTHOR CONTRIBUTIONS

SS analyzed the data, designed the study, and wrote the first version of the manuscript and created graphics and tables. JH designed the NUMEX Experiment and collected the branch samples. AB and JH contributed in designing the experiment, writing of the manuscript, and interpretation of data and results.

FUNDING

The German Research Foundation (DFG) supported this study by funding the project BR 1895/14-2 (FOR 816) and BR 1895/23-1 (PAK 823).

ACKNOWLEDGMENTS

We acknowledge Nina Helmschrott for assistance in carrying out thin-sections and Cathrin Meinardus and Franziska Volland for constructive and fruitful discussions. We also thank Naturaleza y Cultura Internacional (NCI, Loja, Ecuador) for their help in accessing the “Reserva San Francisco.”

REFERENCES

- Arnold, D., and Mauseth, J. (1999). Effects of environmental factors on development of wood. *Am. J. Bot.* 86, 367–371. doi: 10.2307/2656758
- Barnett, J., Gril, J., and Saranpää, P. (2014). “Introduction,” in *The Biology of Reaction Wood*. Springer Series in Wood Sciences, eds B. Gardiner, J. Barnett, P. Saranpää, and J. Gril (Berlin; Heidelberg: Springer), 1–11.
- Beck, E., and Richter, M. (2008). “Ecological aspects of biodiversity hotspot in the Andes of Southern Ecuador,” in *The Tropical Mountain Forest. Pattern and Processes in a Biodiversity Hotspot*. Biodiversity and Ecology Series, Vol. 2, eds R. Gradstein, J. Homeier and D. Gansert (Göttingen: Universitätsverlag), 195–217.
- Bühl, A. (2008). *SPSS 16. Einführung in Die Moderne Datenanalyse, 11th Edn*. München: Pearson Studium.
- Carlquist, S. (1977). Ecological factors in wood evolution. A floristic approach. *Am. J. Bot.* 64, 887–896.
- Carlquist, S. (1984). Vessel grouping in dicotyledon wood: significance and relationship to imperforate tracheary vessel elements. *ALISO* 10, 505–525.
- Carlquist, S. (2001). *Comparative Wood Anatomy – Systematic, Ecological, and Evolutionary Aspects of Dicotyledon Wood, 2nd Edn*. Berlin: Springer.
- Cavelier, J., Tanner, E., and Santamaria, J. (2000). Effect of water, temperature and fertilizer on soil nitrogen net transformations and tree growth in an Elfin cloud forest of Colombia. *J. Trop. Ecol.* 16, 83–99. doi: 10.1017/S0266467400001280
- Chavarrí, B., and León, W. (2005). Estudio anatómico del xilema secundario en siete especies de la subfamilia alyphoideae (euphorbiaceae) en venezuela. *Acta Bot. Venez.* 28, 233–256.
- Cochard, H., Höllta, T., Herbet, S., Delzon, S., and Mencuccini, M. (2009). New insights into the mechanisms of water-stress-induced cavitation in conifers. *Plant Physiol.* 151, 949–954. doi: 10.1104/pp.109.138305
- Etzold, H. (2002). Simultanfärbung von Pflanzenschnitten mit Fuchsin, Chrysoidin und Astrablau. *Mikrokosmos* 91, 316–318.
- Fan, Z.-X., Zhang, S.-B., Gunag-You, H., Ferry Slik, J. W., and Cao, K.-F. (2012). Hydraulic conductivity traits predict growth rates and adult stature of 40 Asian tropical tree species better than wood density. *J. Ecol.* 100, 732–741. doi: 10.1111/j.1365-2745.2011.01939.x
- Faustino, L., Bulfe, N., Pinazo, M., Monteoliva, S., and Graciano, C. (2013). Dry weight partitioning and hydraulic traits in young *Pinus taeda* trees fertilized with nitrogen and phosphorus in a subtropical area. *Tree Physiol.* 33, 242–251. doi: 10.1093/treephys/tps129
- Fichtler, E., and Worbes, M. (2012). Wood anatomical variables in tropical trees and their relation to site conditions and individual tree morphology. *IAWA J.* 33, 119–140. doi: 10.1163/22941932-90000084
- Filho, M., Lisi, C., Hansen, N., and Cury, C. (2004). Anatomical features of increment zones in different tree species in the State of São Paulo, Brasil. *Sci. For.* 66, 46–55.
- Fisher, J., Malhi, Y., Torres, I., Metcalfe, D., van de Weg, M., Meir, P., et al. (2013). Nutrient limitation to rainforests and cloud forest along a 3000m elevation gradient in the Peruvian Andes. *Oecologia* 172, 889–902. doi: 10.1007/s00442-012-2522-6
- Fonti, P., von Arx, G., Garcia-Gonzales, I., Eilmann, B., Sass-Klassen, U., Gärtner, H., et al. (2010). Studying global change through investigation of the plastic responses of xylem anatomy in tree rings. *New Phytol.* 185, 42–53. doi: 10.1111/j.1469-8137.2009.03030.x
- Fournier, M., Alméras, T., Clair, B., and Gril, J. (2014). “Biochemical action and biological function” in *The Biology of Reaction Wood*. Springer Series in Wood Sciences, eds B. Gardiner, J. Barnett, P. Saranpää, and J. Gril (Berlin, Heidelberg: Springer), 1–11.
- Galloway, J., Aber, J., Erisman, J., Seitzinger, S., Howarth, R., Cowling, E., et al. (2003). The nitrogen cascade. *Bioscience* 53, 341–356. doi: 10.1641/0006-3568(2003)053[0341:TNC]2.0.CO;2
- Galloway, J. N., Townsend, A. R., Erisman, J. W., Bekunda, M., Cai, Z., Freney, J. R., et al. (2008). Transformation of the nitrogen cycle: recent trends, questions, and potential solutions. *Science* 320, 889–892. doi: 10.1126/science.1136674
- Goldstein, G., Bucci, S., and Scholz, F. (2013). Why do trees adjust water relations and hydraulic conductivity in response to nutrient availability? *Tree Physiol.* 33, 238–240. doi: 10.1093/treephys/tp007
- Hacke, U. (2015). *Functional and Ecological Xylem Anatomy*. Cham; Heidelberg: New York, NY: Springer.
- Hacke, U., Plavoka, L., Almeida-Rodriguez, A., King-Jones, S., Zhou, W., and Cooke, J. (2010). Influence of nitrogen fertilization on xylem traits and aquaporin expression in stems of hybrid poplar. *Tree Physiol.* 30, 1016–1025. doi: 10.1093/treephys/tpq058
- Hacke, U., Sperry, J., Wheeler, J., and Castro, L. (2006). Scaling of Angiosperm xylem structure with safety and efficiency. *Tree Physiol.* 26, 689–701. doi: 10.1093/treephys/26.6.689
- Harvey, H., and Van den Driessche (1997). Nutrition, xylem cavitation and drought resistance in hybrid poplar. *Tree Physiol.* 17, 647–654. doi: 10.1093/treephys/17.10.647
- Hedin, L., Brookshire, E., Menge, D., and Barron, A. (2009). The nitrogen paradox in tropical forest ecosystems. *Annu. Rev. Ecol. Evol. Syst.* 40, 613–635. doi: 10.1146/annurev.ecolsys.37.091305.110246
- Hoerber, S., Leuschner, C., Köhler, L., Arias-Aguilar, D., and Schuldt, B. (2014). The importance of hydraulic conductivity and wood density to growth performance in eight tree species from a tropical semi-dry climate. *Forest. Ecol. Manag.* 330, 126–136. doi: 10.1016/j.foreco.2014.06.039
- Homeier, J., Breckle, S. W., Günter, S., Rollenbeck, R. T., and Leuschner, C. (2010). Tree diversity, forest structure and productivity along altitudinal and topographical gradients in a species-rich Ecuadorian montane rain forest. *Biotropica* 42, 140–148. doi: 10.1111/j.1744-7429.2009.00547.x
- Homeier, J., Hertel, D., Camenzind, T., Cumbicus, N. L., Maraun, M., Martinson, G. O., et al. (2012). Tropical Andean forests are highly susceptible to nutrient inputs—rapid effects of experimental N and P Addition to an ecuadorian montane forest. *PLoS One* 7:e47128. doi: 10.1371/journal.pone.0047128
- Homeier, J., Leuschner, C., Bräuning, A., Cumbicus, N., Hertel, D., Martinson, G., et al. (2013). “Effects of nutrient addition on the productivity of montane forests and implications for the carbon cycle,” in *Ecosystem Services, Biodiversity and Environmental Change in a Tropical Mountain Ecosystem of South Ecuador, Ecological Studies*, Vol. 221, eds J. Bendix, E. Beck, A. Bräuning, F. Makeschin, R. Mosandl, S. Scheu, and W. Wilcke (Berlin; Heidelberg: Springer), 315–329.
- Homeier, J., and Werner, F. A. (2008). “Spermatophyta. checklist of the reserva biológica San Francisco (Prov. Zamora-Chinchipe, S-Ecuador),” in *Provisional Checklists of Flora and Fauna of the San Francisco Valley and Its Surroundings. Ecotropical Monographs 4*, eds S. Liede-Schumann and S. W. Breckle (Hamburg: Society for Tropical Ecology), 15–58.
- Lachenbruch, B., and McCulloh, K. (2014). Traits, properties, and performance: how woody plants combine hydraulic and mechanical functions in a cell, tissue, or whole plant. *New Phytol.* 204, 747–764. doi: 10.1111/nph.13035
- Mayor, J. R., Wright, S. J., and Turner, B. L. (2014). Species-specific responses of foliar nutrients to long-term nitrogen and phosphorus additions in a lowland tropical forest. *J. Ecol.* 102, 36–44. doi: 10.1111/1365-2745.12190
- McCulloh, K., Meinzer, F., Sperry, J., Lachenbruch, B., Voelker, S., Woodruff, D., et al. (2011). Comparative hydraulic architecture of tropical tree species representing a range of successional stages and wood density. *Oecologia* 167, 27–37. doi: 10.1007/s00442-011-1973-5
- McCulloh, K., Sperry, J., Lachenbruch, B., Meinzer, F., Reich, P., and Voelker, S. (2010). Moving water well. Comparing hydraulic efficiency in twigs and trunks of coniferous, ring-porous, and diffuse-porous saplings from temperate and tropical forests. *New Phytol.* 186, 439–450. doi: 10.1111/j.1469-8137.2010.03181.x
- Meinzer, F., Campanello, P., Domec, J. C., Genoeca Gatti, M., Goldstein, G., Villalobos-Vega, R., et al. (2008). Constraints on physiological function associated with branch architecture and wood density in tropical forest trees. *Tree Physiol.* 28, 1609–1617. doi: 10.1093/treephys/28.11.1609
- Meinzer, F., McCulloh, K., Lachenbruch, B., Woodruff, D., and Johnson, D. (2010). The blind men and the elephant: the impact of context and scale in evaluating conflicts between plant hydraulic safety and efficiency. *Oecologia* 164, 287–296. doi: 10.1007/s00442-010-1734-x
- Oladi, R., Bräuning, A., and Pourtahmasi, K. (2014). “Plastic” and “static” behavior of vessel-anatomical features in Oriental beech (*Fagus orientalis* Lipsky) in view of xylem hydraulic conductivity. *Trees* 28, 493–502. doi: 10.1007/s00468-013-0966-x
- Pittermann, J. (2010). The evolution of water transport in plants: an integrated approach. *Geobiology* 8, 112–139. doi: 10.1111/j.1472-4669.2010.00232.x

- Poorter, H., Niinemets, U., Poorter, L., Wright, I., and Villar, R. (2009). Causes and consequences of variation in leaf mass per area (LMA): a meta-analysis. *New Phytol.* 182, 565–588. doi: 10.1111/j.1469-8137.2009.02830.x
- Powers, J., Becklund, K., Gei, M., Siddharth, I., Meyer, R., O'Connell, C., et al. (2015). Nutrient addition effects on tropical dry forests: a mini review from microbial to ecosystem Scales. *Front Earth Sci.* 3:34. doi: 10.3389/feart.2015.00034
- Richter, M., Beck, E., and Rollenbeck, J., Bendix (2013). "The study area," in *Ecosystem Services, Biodiversity and Environmental Change in a Tropical Mountain Ecosystem of South Ecuador, Ecological Studies*, Vol. 221, eds J. Bendix, E. Beck, A. Bräuning, F. Makeschin, R. Mosandl, S. Scheu, and W. Wilcke, (Berlin; Heidelberg: Springer), 3–17.
- Rollenbeck, J., and Bendix, J. (2011). Rainfall distribution in the Andes of southern Ecuador derived from blending weather radar data and meteorological field observations. *Atmos. Res.* 99, 227–289. doi: 10.1016/j.atmosres.2010.10.018
- Scholz, A., Kleptsch, M., Karimi, Z., and Jansen, S. (2013). How to quantify conduits in wood? *Front. Plant Sci.* 4:56. doi: 10.3389/fpls.2013.00056
- Schuldt, B. (2005). *Untersuchungen zum Wasserhaushalt tropischer Bäume in Abhängigkeit von der Meereshöhe in Süd-Ecuador*. Unpublished diploma thesis, University of Göttingen, Germany.
- Schuldt, B., Leuschner, C., Brock, N., and Horna, V. (2013). Changes in wood density, wood anatomy and hydraulic properties of the xylem along the root to shoot flow path of tropical rainforest trees. *Tree Physiol.* 33, 161–174. doi: 10.1093/treephys/tps122
- Secco, R. S. (2008). *Alchornea lojaensis*, a new species of Euphorbiaceae for the Flora of Ecuador. *Kew Bull.* 63, 511–513. doi: 10.1007/s12225-008-9043-9
- Smil, V. (2000). Phosphorous in the environment: natural flows and human interfaces. *Annu. Rev. Energy Environ.* 25, 53–88. doi: 10.1146/annurev.energy.25.1.53
- Smith, M., Fridley, J., Jinghing, Y., and Bauerle, T. (2013). Contrasting xylem vessel constraints on hydraulic conductivity between native and non-native woody understory species. *Front. Plant Sci.* 4:486. doi: 10.3389/fpls.2013.00486
- Spannl, S., Ganzhi, O., Peter, T., and Bräuning, A. (2013). "Tree growth under climatic and trophic forcing — a nutrient manipulation experiment in Southern Ecuador," in *Proceedings of the DENDROSYMPOSIUM 2012: May 8th – 12th, 2012 in Potsdam and Eberswalde, Germany (Scientific Technical Report; 13/05), 11th TRACE Conference (Tree Rings in Archaeology, Climatology and Ecology) (Potsdam and Eberswalde 2012)*, eds G. Helle, H. Gärtner, W. Beck, I. Heinrich, K.-U. Heußner, A. Müller, and T. Sanders (Potsdam: Deutsches GeoForschungsZentrum), 14–19. doi: 10.2312/GFZ.b103-13058
- Sperry, J., Meinzer, F., and McCulloh, K. (2008). Safety and efficiency conflicts in hydraulic architecture: scaling from tissues to trees. *Plant Cell Environ.* 31, 632–645. doi: 10.1111/j.1365-3040.2007.01765.x
- Tanaka, M., Girard, G., Davis, R., Peuto, A., and Bignell, N. (2001). Recommended table for the density of water between 0°C and 40°C based on recent experimental reports. *Metrologia* 38, 301–309. doi: 10.1088/0026-1394/38/4/3
- Tanner, E., Kapos, V., Freskos, S., Healey, J., and Theobald, A. (1990). Nitrogen and phosphorous fertilization of Jamaican montane forest trees. *J. Trop. Ecol.* 6, 231–238. doi: 10.1017/S0266467400004375
- Tyree, M., and Zimmermann, M. (2002). *Xylem Structure and the Ascent of Sap, 2nd Edn*. Berlin; Heidelberg; New York, NY: Springer-Verlag.
- Vitousek, P., Porder, S., Houlton, B., and Chadwick, O. (2010). Terrestrial phosphorous limitation: mechanisms, implications, and nitrogen-phosphorous interactions. *Ecol. Appl.* 20, 5–15. doi: 10.1890/08-0127.1
- von Arx, G., Kueffer, C., and Fonti, P. (2013). Quantifying plasticity in vessel grouping – added value from the image analysis tool roxas. *IAWA J.* 34, 433–445. doi: 10.1163/22941932-00000035
- Wheeler, E. (1986). Vessel per square millimeter or vessel groups per square millimeter? *IAWA Bull.* 7, 73–74.
- Wheeler, E., Baas, P., and Gasson, P. (1989). IAWA list of microscopic features for hardwood identification. *IAWA Bull.* 10, 219–332.
- Wilcke, W., Yasin, S., Abramowski, U., Valarezo, C., and Zech, W. (2002). Nutrient storage and turnover in organic layers under tropical montane rain forest in Ecuador. *Eur. J. Soil Sci.* 53, 15–27. doi: 10.1046/j.1365-2389.2002.00411.x
- Worbes, M. (1995). How to measure growth dynamics in tropical trees. A review. *IAWA J.* 16, 337–351. doi: 10.1163/22941932-90001424
- Wright, I. J., Reich, P. B., Westoby, M., Ackerly, D. D., Baruch, Z., Bongers, F., et al. (2004). The worldwide leaf economics spectrum. *Nature* 428, 821–827. doi: 10.1038/nature02403
- Wright, S. (2005). Tropical forests in a changing environment. *Trends Ecol. Evol.* 20, 553–560. doi: 10.1016/j.tree.2005.07.009
- Zach, A., Schuldt, B., Horna, V., Tjitrosemito, S., and Leuschner, C. (2010). "The hydraulic performance of tropical rainforest trees in their perhumid environment. Is there evidence for drought vulnerability?" in *Tropical Rainforests and Agroforests under Global Change*, eds T. Tschardt, C. Leuschner, E. Veldkamp, H. Faust, E. Guhardja, and A. Bidin (Berlin: Springer), 391–410.
- Zanne, A., Westoby, M., Falster, D., Ackerly, D., Loarie, S., Arnold, S., et al. (2010). Angiosperm wood structure: global patterns in vessel anatomy and their relationship to wood density and potential conductivity. *Am. J. Bot.* 97, 207–215. doi: 10.3732/ajb.0900178
- Zimmermann, M. (1978). Hydraulic architecture of some diffuse-porous trees. *Can. J. Bot.* 56, 2286–2295.
- Zuidema, P., Baker, P., Groenendijk, P., Schippers, P., van der Sleen, P., Vlam, M., et al. (2013). Tropical forests and global change: filling knowledge gaps. *Trends Plant Sci.* 18, 413–319. doi: 10.1016/j.tplants.2013.05.006

Conflict of Interest Statement: The authors declare that the research was conducted in the absence of any commercial or financial relationships that could be construed as a potential conflict of interest.

Copyright © 2016 Spannl, Homeier and Bräuning. This is an open-access article distributed under the terms of the Creative Commons Attribution License (CC BY). The use, distribution or reproduction in other forums is permitted, provided the original author(s) or licensor are credited and that the original publication in this journal is cited, in accordance with accepted academic practice. No use, distribution or reproduction is permitted which does not comply with these terms.